frontiers | Frontiers in Chemistry

TYPE Original Research
PUBLISHED 06 December 2024
DOI 10.3389/fchem.2024.1507905

OPEN ACCESS

EDITED BY
Fagen Wang,
Jiangsu University, China

REVIEWED BY
Tianyan Jiang,
Chongqing University of Technology, China
Zixin Wang,
Los Alamos National Laboratory (DOE), United States
Weigen Chen,
Chongqing University, China

*CORRESPONDENCE
Qu Zhou,
zhouqu@swu.edu.cn

RECEIVED 08 October 2024
ACCEPTED 05 November 2024
PUBLISHED 06 December 2024

CITATION
Jiang J, Yang D, Zeng W, Wang Z and Zhou Q (2024) Novel gas sensing mechanisms of Pd and Rh-doped h-BN monolayers for detecting dissolved gases (H_2、CH_4、and C_2H_4) in transformer oil.
Front. Chem. 12:1507905.
doi: 10.3389/fchem.2024.1507905

Novel gas sensing mechanisms of Pd and Rh-doped h-BN monolayers for detecting dissolved gases (H_2、CH_4、and C_2H_4) in transformer oil

Jiaming Jiang[1], Dingqian Yang[2], Wen Zeng[3], Zhongchang Wang[4] and Qu Zhou[1]*

[1]College of Engineering and Technology, Southwest University, Chongqing, China, [2]State Grid Xinjiang Electric Power Research Institute, Urumqi, Xinjiang, China, [3]College of Materials Science and Engineering, Chongqing University, Chongqing, China, [4]Department of Quantum and Energy Materials, International Iberian Nanotechnology Laboratory (INL), Braga, Portugal

Detecting dissolved gases in transformer oil is crucial for assessing the operational status of transformers. The gas composition in transformer oil can reflect the health status of the equipment and help identify potential failure risks in a timely manner. Based on density functional theory (DFT), Pd and Rh atoms were doped into the h-BN monolayer, and the most stable adsorption structures for each were first explored. Then, the sensing performance of the Pd-doped and Rh-doped h-BN monolayers for H_2, CH_4, and C_2H_4 gases was analyzed. The results indicate that Pd-BN and Rh-BN exhibit enhanced sensitivity to H_2 and C_2H_4 gases compared to pristine h-BN. However, they show poor adsorption characteristics for CH_4. Both Pd-BN and Rh-BN demonstrate strong chemisorption for H_2 and C_2H_4. In contrast, CH_4 adsorption is predominantly physisorbed. The desorption time of H_2 from Pd-BN at 398 K is 164 s, reflecting its excellent desorption performance. Additionally, Pd-BN and Rh-BN monolayers exhibit exceptional C_2H_4 capture capabilities, with adsorption energies of −1.697 eV and −2.188 eV, respectively, indicating their potential as C_2H_4 gas adsorbents. These findings provide theoretical insights for selecting materials for dissolved gas detection in oil and lay the groundwork for the development of Pd-BN and Rh-BN-based gas sensors.

KEYWORDS

Pd-BN, Rh-BN, sensing performance, dissolved gases in transformer oil, DFT

Introduction

Oil-immersed transformers, as a crucial component in the power system, have their operational status directly affecting the stability of the power system (Mu et al., 2022). However, over extended periods of operation, oil-immersed transformers often experience issues such as overheating faults, aging faults, and partial discharge faults (Peng et al., 2023; Long et al., 2024). The insulating oil within transformers can be affected, leading to the generation of fault characteristic gases dissolved in the oil, such as hydrogen (H_2) and various low molecular weight hydrocarbons, including methane (CH_4) and ethylene (C_2H_4) (Zhang et al., 2019; Chen et al., 2022; Li B. L. et al., 2022; Wu et al., 2024). Thermal faults, aging faults, and partial discharge faults not only pose serious threats to the safe operation

and service life of transformers but also impact the performance of the insulation, leading to its degradation (Bustamante et al., 2019; Wang et al., 2021; Manoj et al., 2023; Jiang et al., 2024). Therefore, timely detection of these faults in transformers is crucial. As the internal insulation condition of oil-immersed transformers changes and insulation failure intensifies, the types, quantities, and the rates of generation of fault characteristic gases dissolved in the insulation oil also vary accordingly (Du et al., 2018; Zhou et al., 2023). Therefore, analyzing the composition and concentration of fault characteristic gases in the oil aids in assessing the condition of internal insulation faults and predicting the operational status of the transformer (Elele et al., 2022; Ali et al., 2023; Zhong et al., 2023).

Two-dimensional nanomaterials have recently become a focal point in gas sensor research due to their high specific surface area, enhanced chemical reactivity, and excellent carrier mobility. These attributes make them particularly promising for advancing sensor technology (Jiang et al., 2024; Kumar et al., 2024; Long et al., 2024; Zhang et al., 2024). Furthermore, the application of sensors based on two-dimensional nanomaterials for detecting dissolved gases in transformer oil has been extensively studied (Zhou et al., 2018; Li Z. H. et al., 2022; Mishra et al., 2022; Hussein et al., 2023; Gao M. Y. et al., 2024). h-BN is a typical graphene-like material that, compared to conventional graphene, exhibits superior thermal stability and chemical stability (Wang et al., 2017; Ngamprapawat et al., 2023; Ogawa et al., 2023). Pd and Rh have attracted significant attention due to their excellent carrier mobility and outstanding catalytic performance in gas interactions. They are considered suitable dopant metals for enhancing surface properties (Oyo-Ita et al., 2023; Sun et al., 2023; Gao G. et al., 2024; Yao et al., 2024; Yu et al., 2024). Doping transition metal atoms such as Pd and Rh can significantly enhance the material's reactivity and gas transport capabilities (Kou et al., 2018; Zhao and Wu, 2018; Ni et al., 2020; Peng et al., 2021; Du and Wu, 2022). Based on this, it is anticipated that doping with Pd and Rh atoms could improve the adsorption characteristics of monolayer h-BN towards dissolved characteristic gases in transformer oil, thereby facilitating the detection of these gases. However, research on the gas-sensing mechanisms of Pd and Rh-doped h-BN monolayers in relation to dissolved characteristic gases in oil is still limited.

This study investigates the use of Pd and Rh transition metal atoms doped separately into monolayer h-BN as sensing materials for H_2, CH_4, and C_2H_4. Based on first-principles density functional theory (DFT), the adsorption processes of Rh-doped and Pd-doped h-BN monolayers are calculated and analyzed. DFT calculations have been extensively utilized in previous research within the field of sensing properties. Therefore, this study contributes to the development of gas sensors for detecting dissolved gases in transformer oil. The findings from this research not only advance our understanding of gas adsorption mechanisms but also have significant implications for enhancing the safety and reliability of power systems. By improving the detection of dissolved gases in transformer oil, this study contributes to the development of more effective fault detection technologies, ultimately promoting the stability and efficiency of electrical infrastructures.

Parameter settings

All theoretical calculations in this study were performed using the DMol3 package within Materials Studio (MS) based on Density Functional Theory (DFT). We employed the Perdew–Burke–Ernzerhof (PBE) functional within the Generalized Gradient Approximation (GGA) to describe exchange-correlation potentials (Wang et al., 2024). To more accurately capture long-range interactions and van der Waals forces, the semi-empirical dispersion correction method (DFT-D) proposed by Grimme was used to account for van der Waals interactions (Grimme, 2006). The calculations utilized a Double Numerical with Polarization (DNP) atomic orbital basis set to ensure high computational quality and employed DFT semi-core pseudopotentials (DSPP) for Pd and Rh atoms to handle relativistic effects (Zeng et al., 2020). For geometry optimization, a 3 × 3 × 1 Monkhorst–Pack grid was used for k-point sampling in the Brillouin zone. The convergence criteria were set as: maximum force, maximum displacement, and energy tolerance of 0.002 Ha/Å, 0.005 Å, and 10^{-5} Ha, respectively. The self-consistent field (SCF) convergence threshold for static electronic structure calculations was set to 10^{-6} Ha, with a Gaussian broadening Sigma parameter of 0.005 Ha to ensure accuracy in total energy results. The smearing value for thermal broadening effects is set to 0.005 Ha. A 4 × 4 × 1 supercell of the h-BN monolayer was constructed, with a 15 Å vacuum region to avoid interactions between adjacent supercells. The optimized lattice constant of the h-BN monolayer was 2.5 Å, consistent with other theoretical values.

To determine the most stable doping structure, we employed the binding energy equation. Formula 1 can be used to calculate the binding energies (E_b) of Rh and Pd atoms at each site of the h-BN monolayer (Chen et al., 2024).

$$E_b = E_{ATOM-BN} - E_{ATOM} - E_{BN} \tag{1}$$

Where $E_{ATOM-BN}$、 E_{ATOM} and E_{BN} represent the total energy of the Rh or Pd doped complex, the Rh or Pd atom, and the undoped BN, respectively. Typically, a negative binding energy E_b indicates a spontaneous exothermic reaction.

The adsorption energy E_{ads} can reflects the energy change of the entire adsorption system, allowing for the assessment of the strength of the adsorption reaction, the specific expression is shown in Formula 2 (Yu et al., 2024):

$$E_{ads} = E_{gas-sub} - E_{sub} - E_{gas} \tag{2}$$

Where $E_{gas-sub}$, E_{sub} and E_{gas} stands for the total energy of the adsorption system, the energy of gas-sensitive material and gas molecule, respectively. When $E_{ads} < 0$, it indicates that the adsorption reaction is exothermic and chemical, making it spontaneous. If the absolute value of the $E_{ads} > 0.8$ eV, it can be considered strong chemical adsorption. Conversely, when $E_{ads} > 0$, it indicates that the adsorption reaction is endothermic and physical, and thus not spontaneous.

The amount of charge transfer can reflect the change in the charge carried by gas molecules before and after the adsorption reaction, thus allowing the assessment of the impact of the adsorption reaction on the electrical conductivity of gas-sensitive materials. This can be expressed by Formula 3 (Tang et al., 2020):

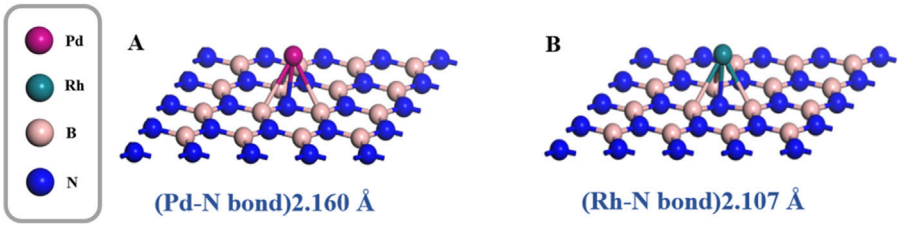

FIGURE 1
Geometric structure of **(A)** Pd-BN, **(B)** Rh-BN.

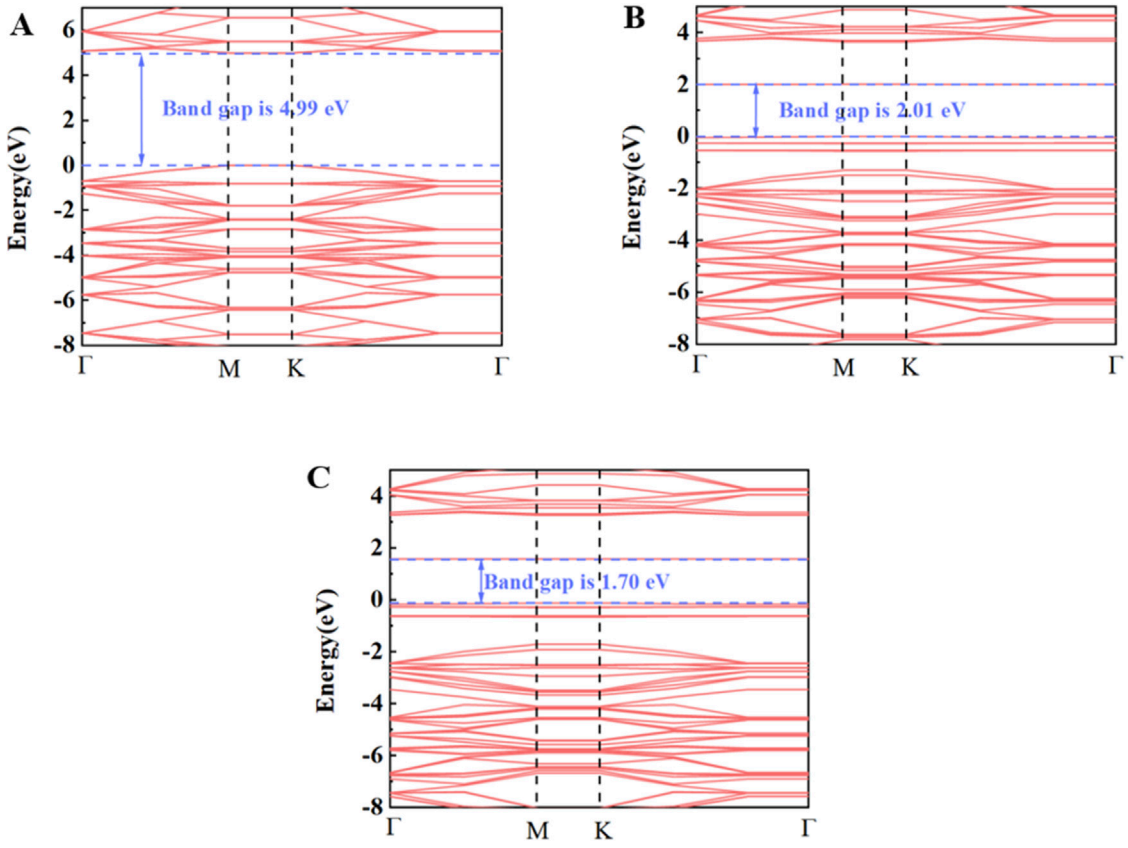

FIGURE 2
Band structure of **(A)** h-BN, **(B)** Pd-BN, **(C)** Rh-BN.

$$Q_t = Q_a - Q_b \quad (3)$$

Where Q_a and Q_b denote the amount of charge carried by gas molecules after adsorption and the amount of charge carried before adsorption.

Results and discussion

Establishment of the doping model

To determine the optimal doping structure of Pd and Rh atoms on a single layer of h-BN, we considered doping at four distinct sites: atop N atoms (TN), atop B atoms (TB), at the midpoint of B-N bonds (TM), and at the center of the BN hexagons (TH). By comparing the binding energies (E_b) of each doping configuration at these sites, we found that the most stable doping structure for both Pd and Rh atoms is at the TN site, where both exhibit the lowest binding energy and adsorption distance.

The optimized geometric models of Pd-doped and Rh-doped h-BN monolayers are shown in Figure 1. The binding energies for the two structures are −1.123 eV and −1.396 eV, respectively, with Pd and Rh atoms located at distances of 2.160 Å and 2.107 Å from the N atoms. Additionally, compared to the intrinsic band gap of h-BN (4.988 eV) (Guo et al., 2022), the band gaps of Pd-doped BN and Rh-doped BN are significantly reduced to 2.055 eV and

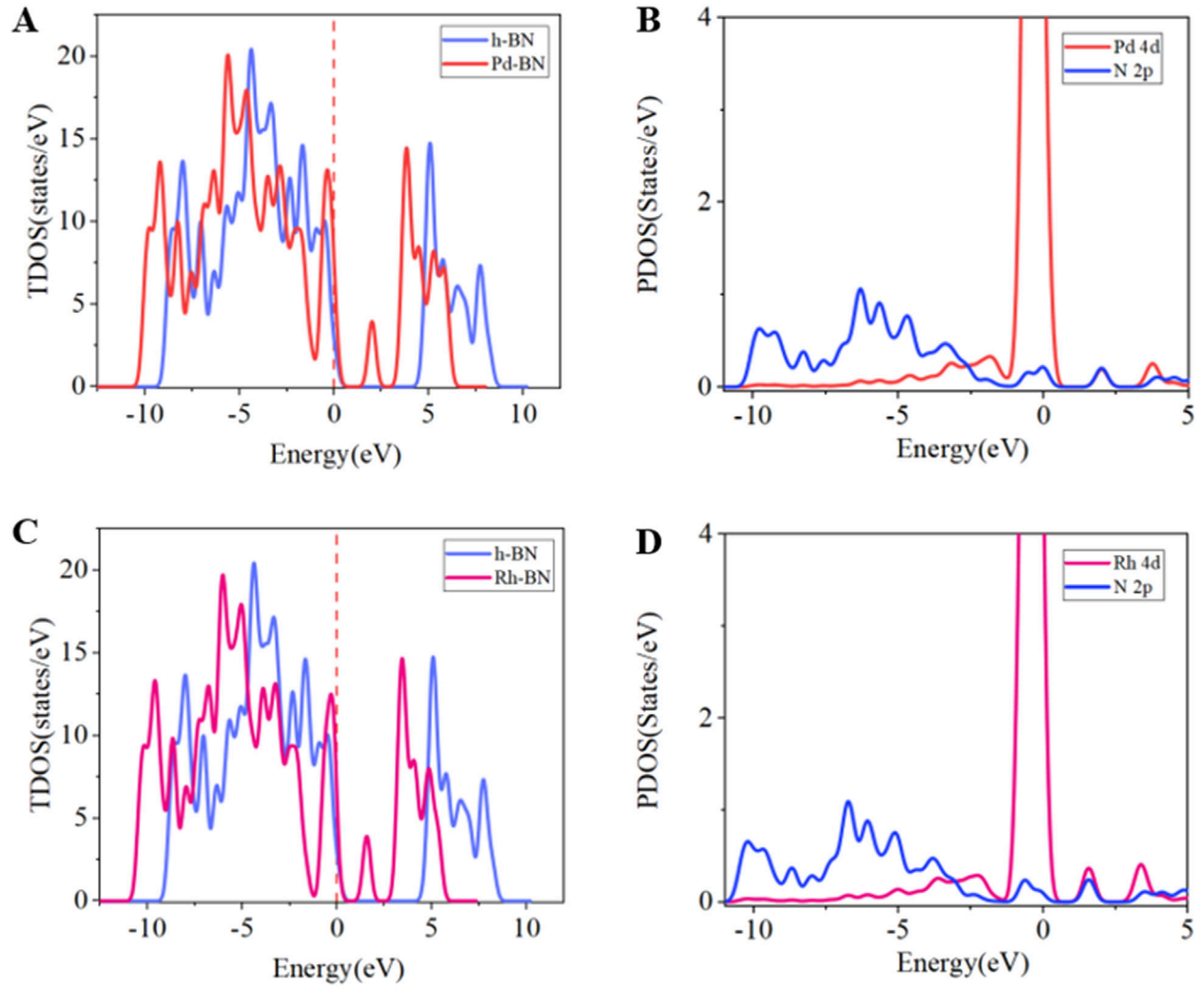

FIGURE 3
(A) TDOS of h-BN and Pd-BN, **(B)** PDOS of Pd-BN, **(C)** TDOS of h-BN and Rh-BN, **(D)** PDOS of Rh-BN.

1.697 eV, respectively. The band gap diagrams are presented in Figure 2. These results indicate that both Pd and Rh atoms significantly enhance the electrical conductivity of the monolayer, demonstrating effective doping.

To further analyze the electronic behavior of Pd-BN monolayers, Rh-BN monolayers, and pure h-BN monolayers, we performed total density of states (TDOS) analysis for all three systems. The results indicate a significant contribution of Pd and Rh atoms to the TDOS. In both Pd-BN and Rh-BN systems, new peaks appear to the right of the Fermi level, suggesting that electron transfer from the valence band to the conduction band has become easier, consistent with the observed reduction in band gap. Additionally, data presented in Figure 3B reveal substantial overlap between Pd 4d and N 2p orbitals within the range of −10.5 eV–5 eV, highlighting strong hybridization between Pd atoms and the BN layer. Similarly, Figure 3D shows notable overlap between Rh 4d and N 2p orbitals, indicating a strong bonding interaction between Rh atoms and h-BN. These analyses underscore the impact of Pd and Rh atoms on the electronic behavior of the BN layer and their significant modification of the material's electronic structure.

TABLE 1 Adsorption parameters of the Pd-BN monolayer and Rh-BN monolayer to dissolved gases in transformer oil.

Gas	Model	E_{ads} (eV)	Q_t (e)	D(Å)	Bandgap (eV)
H_2	Pd-BN	−1.123	−0.044	1.736	3.421
	Rh-BN	−1.516	−0.027	1.686	2.944
CH_4	Pd-BN	−0.121	−0.028	1.968	3.703
	Rh-BN	−0.116	0.028	1.886	3.364
C_2H_4	Pd-BN	−1.697	−0.100	2.157	2.869
	Rh-BN	−2.188	−0.090	2.120	2.601

Adsorption properties

To investigate the sensing and adsorption properties of monolayers of Pd-BN and Rh-BN for H_2, CH_4, and C_2H_4 gases, adsorption models for different adsorption behaviors were established. Optimization calculations yielded the optimal adsorption configurations for these

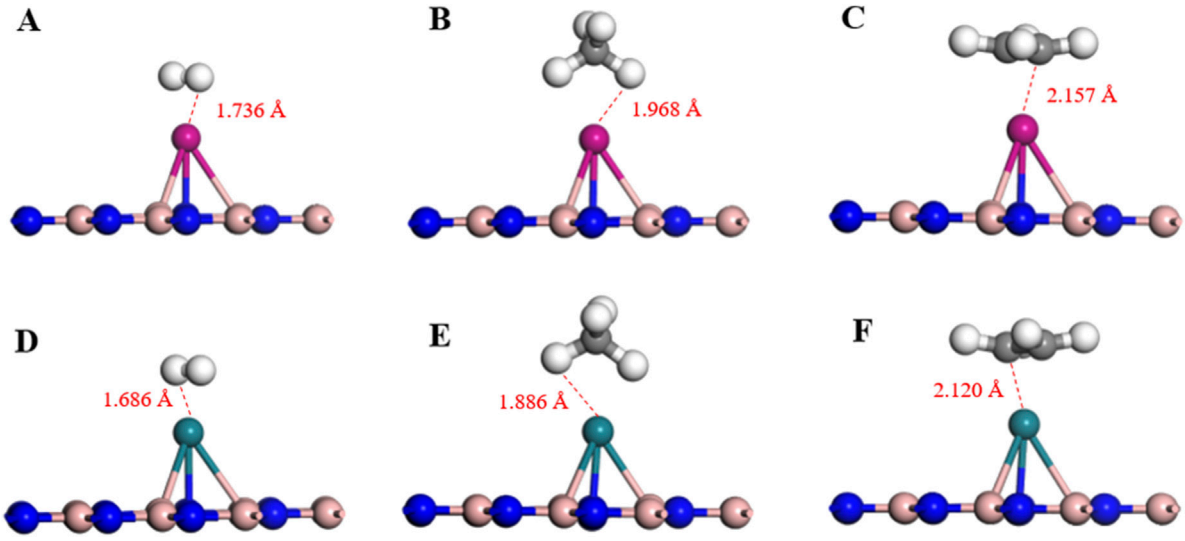

FIGURE 4
The optimal adsorption configuration of **(A)** Pd-BN/H_2, **(B)** Pd-BN/CH_4, **(C)** Pd-BN/C_2H_4, **(D)** Rh-BN/H_2, **(E)** Rh-BN/CH_4, **(F)** Rh-BN/C_2H_4.

gases on both monolayers. The adsorption energies, charge transfers, adsorption distances, and band gaps for the six adsorption systems are summarized in Table 1.

Based on the adsorption parameters presented in Table 1, it can be preliminarily concluded that the Pd-BN monolayer exhibits favorable adsorption properties for H_2 and C_2H_4 molecules, with adsorption energies of −1.123 eV and −1.697 eV, respectively. In contrast, the adsorption of CH_4 molecules is less effective, as evidenced by its relatively low adsorption energy of −0.121 eV. H_2 and C_2H_4 have relatively short adsorption distances on the Pd-BN monolayer, as shown in Figure 4, measuring 1.736 Å and 2.157 Å, respectively. This indicates a strong interaction between H_2, C_2H_4 molecules and the Pd-BN monolayer. The negative adsorption energies suggest that these adsorption processes are spontaneous, with considerable adsorption energy magnitudes. The larger absolute values of the adsorption energies for H_2 and C_2H_4 imply that the adsorption of these molecules on the Pd-BN monolayer is likely chemisorptive. Conversely, the negligible charge transfer for CH_4 suggests that its interaction with the monolayer is primarily a weak physisorption.

Based on the adsorption parameters for H_2, CH_4, and C_2H_4 molecules on the Rh-BN Based on the adsorption parameters of H_2 and C_2H_4 on the Rh-BN monolayer, it is similarly evident that there is a strong interaction between the Rh-BN monolayer and these two gas molecules. The adsorption energy of H_2 on the Rh-BN monolayer is −1.516 eV, and the adsorption distance, as shown in Figure 4D, is 1.686 Å. Indicating a significant interaction between them. Additionally, the Hirshfeld charge distribution method reveals that H_2, acting as an electron donor, contributes 0.027 e to the Rh-BN monolayer, suggesting a notable charge transfer from the H_2 molecule to the Rh-BN monolayer. The adsorption energy and charge transfer for CH_4 are minimal, indicating that CH_4 interacts with the Rh-BN monolayer through weak physisorption. Conversely, the adsorption energy and charge transfer for C_2H_4 are substantial, reflected by the larger adsorption energy and significant charge transfer, suggesting strong chemisorption of C_2H_4 on the Rh-BN monolayer.

Electronic behavior of gas adsorption structures on Pd-BN and Rh-BN based on DOS analysis

To further elucidate the gas-sensing mechanisms and electronic behavior of Pd-BN and Rh-BN monolayers with respect to H_2, CH_4, and C_2H_4 molecules, we analyzed the total density of states (TDOS) and partial density of states (PDOS) of Pd-BN and Rh-BN monolayers under the adsorption of these three gases, as shown in Figure 5.

Firstly, focusing on the TDOS distribution for Pd-BN monolayer in each adsorption system, the red curve represents the TDOS distribution of the bare Pd-BN monolayer, while the blue curve denotes the TDOS distribution after gas adsorption. Significant differences are evident in the TDOS plots for H_2, CH_4, and C_2H_4, both before and after adsorption. Notably, the TDOS near the Fermi level shows substantial changes in the H_2 and CH_4 adsorption systems. The density of states peak of Pd-BN in the range of 1.5 eV–3 eV disappears, making it harder for electrons to transfer from the valence band to the conduction band, consistent with the increase in bandgap observed in Figure 2B. The adsorption of H_2 and CH_4 reduces the electrical conductivity of the Pd-BN monolayer. In the C_2H_4 adsorption system, a shift in the density of states peak to the right of the Fermi level is observed, which also contributes to a certain increase in the bandgap.

In the PDOS curves for the three gas adsorption systems on Pd-BN, overlaps among curves representing different atomic orbitals indicate orbital hybridization. In the H_2 adsorption system shown in Figure 5B, strong hybridization between H 1s and Pd 4d peaks is observed in the ranges of −7.5 eV and 3 eV–6 eV, which corroborates the high adsorption energy of H_2. For the CH_4 adsorption system, despite multiple overlaps between Pd 4d and C 2p, H 1s orbitals, the smaller peak value of Pd 4d indicates less effective adsorption, with physical adsorption being predominant, consistent with the adsorption energy analysis. In the C_2H_4 adsorption system, extensive overlap is observed between −15 eV

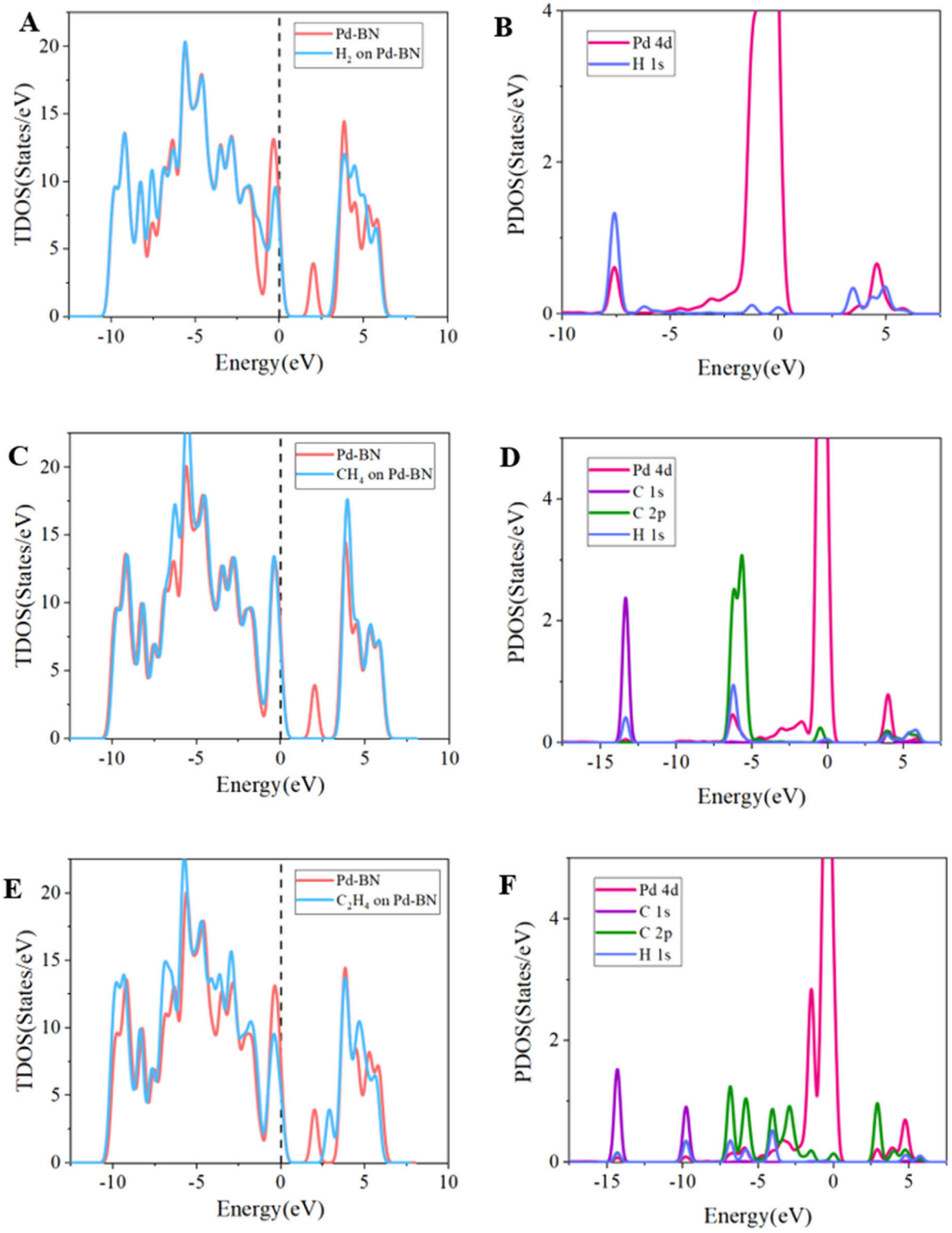

FIGURE 5
Tdos of **(A)** Pd-BN/H_2, **(B)** Pd-BN/CH_4, **(C)** Pd-BN/C_2H_4, PDOS of **(D)** Pd-BN/H_2, **(E)** Pd-BN/CH_4, **(F)** Pd-BN/C_2H_4.

and −2.5 eV, and hybridization occurs between 2.5 eV and 5 eV, indicating strong orbital hybridization between Pd 4d, C 2p, and H 1s orbitals, and strong Pd-C bonding. Additionally, these overlaps significantly deform the TDOS, explaining the shift observed in the TDOS curves. The overlap between Pd 4d and C 2p orbitals in the C_2H_4 adsorption system is greater than that in the H_2 and CH_4 systems, verifying the stronger chemical interaction in the C_2H_4 adsorption system.

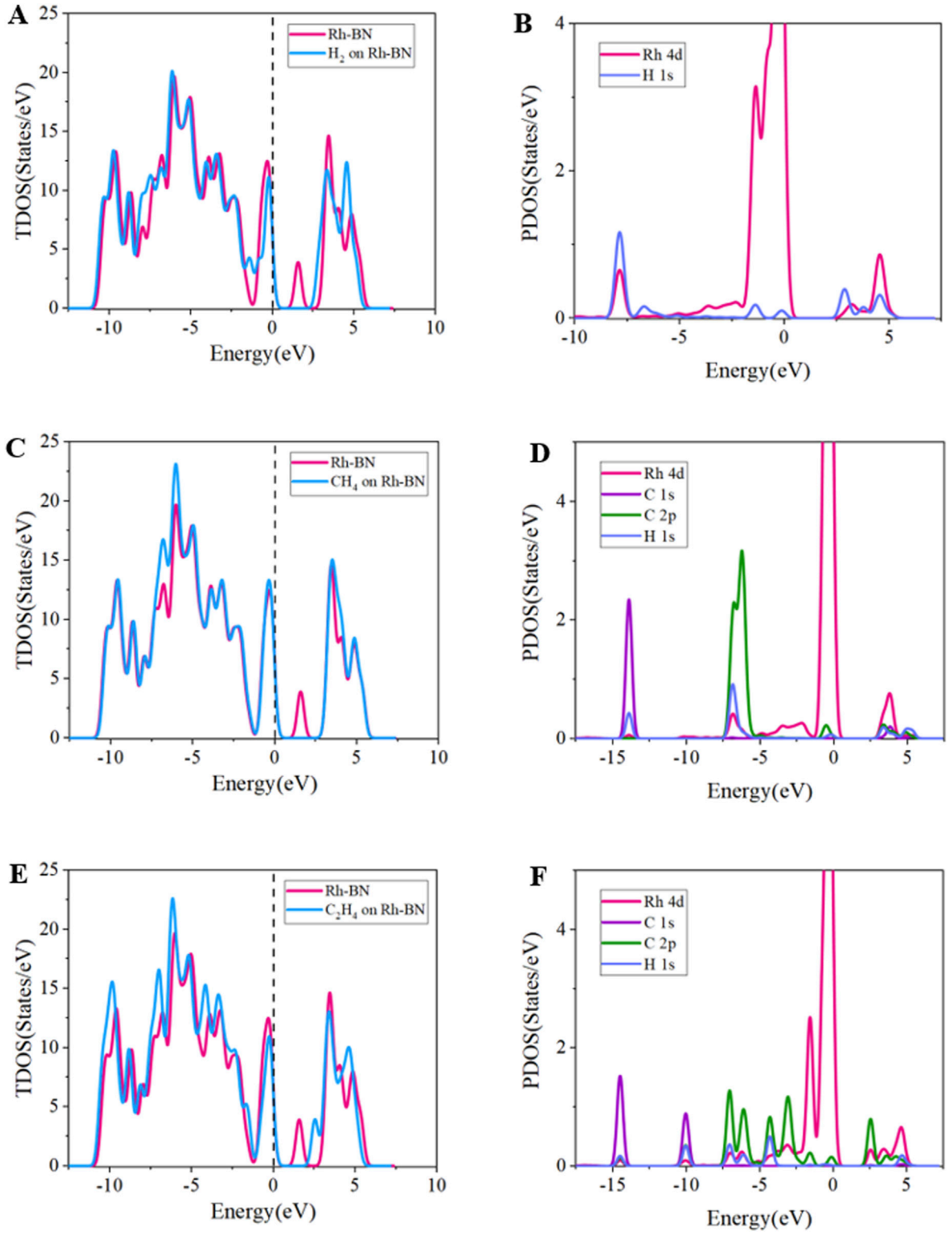

FIGURE 6
Tdos of **(A)** Rh-BN/H_2, **(B)** Rh-BN/CH_4, **(C)** Rh-BN/C_2H_4, PDOS of **(D)** Rh-BN/H_2, **(E)** Rh-BN/CH_4, **(F)** Rh-BN/C_2H_4.

The TDOS and PDOS analysis for the Rh-BN monolayer under adsorption of H_2, CH_4, and C_2H_4 reveals significant changes in electronic structure. As shown in Figure 6, in the H_2 adsorption system, the TDOS shows that the density of states peak on the right side of the Fermi level in the 1 eV–2 eV range disappears, indicating that electron transfer from the valence band to the conduction band becomes more difficult. This observation aligns with the observed increase in bandgap in the adsorption system. For the CH_4

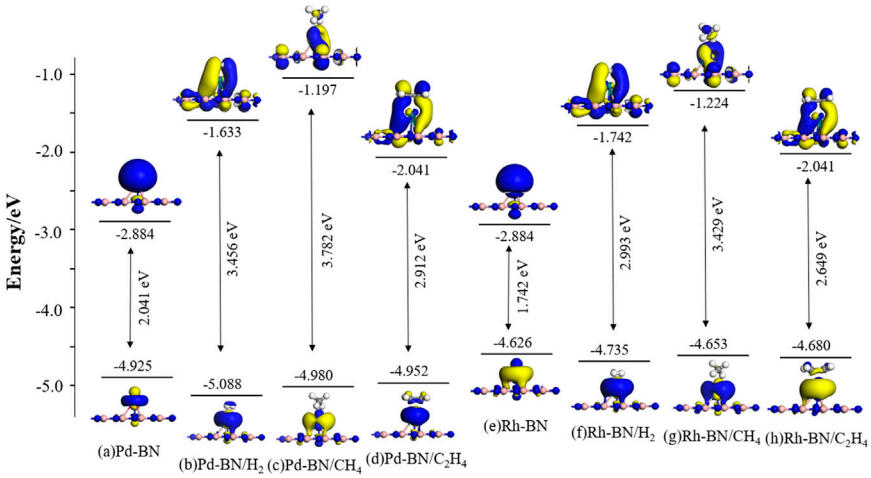

FIGURE 7
Distribution of HOMO and LUMO in Monolayer Pd-BN and Rh-BN and their adsorption systems with three gas molecules.

adsorption system, a similar disappearance of the density of states peak on the right side of the Fermi level occurs, but with considerable curve overlap across a broad range, suggesting that CH_4 adsorption has a minimal impact on the electronic density distribution of Rh-BN. In the C_2H_4 adsorption system, the TDOS shows a notable shift of the density of states peak to higher energy levels compared to the pristine Rh-BN, with an increased intercept width at the fermi level. This implies that C_2H_4 adsorption enlarges the system's bandgap, leading to a downward shift of the Fermi level and decreased electrical conductivity of the Rh-BN monolayer.

The PDOS for Rh-BN/H_2 shows significant overlap between Rh 4d and H 1s orbitals at −8 eV, along with hybridization between 2.5 eV and 5 eV, indicating a strong binding interaction between Rh-BN and H_2. This explains the high adsorption energy and structural stability of the Rh-BN/H_2 system. For Rh-BN/CH_4, the PDOS results show limited orbital overlap between Rh 4d and C 2p, H 1s orbitals at −7.5 eV, reflecting poor adsorption efficacy of CH_4. In the Rh-BN/C_2H_4 system, the PDOS reveals extensive and continuous overlap between Rh 4d and C 2p, H 1s orbitals in the −7.5 eV to −2.5 eV range, signifying strong chemical adsorption of C_2H_4 on the Rh-BN monolayer, consistent with the high E_{ad} value and the stable geometric configuration of the C_2H_4 adsorption system.

Band gap study based on frontier orbital theory

It is generally accepted that the electrical conductivity is related to the band gap through the Formula 4:

$$\sigma \propto \exp\left(\frac{-E_g}{k_B T}\right) \tag{4}$$

Where k_B is the Boltzmann constant, T is the temperature.

From the above equation, it can be seen that the electrical conductivity is inversely proportional to the band gap under certain temperature conditions. In this section, frontier orbital theory is employed to quantitatively assess changes in the band gap by calculating the energies of the highest occupied molecular orbital (HOMO) and the lowest unoccupied molecular orbital (LUMO). This allows for an analysis of how adsorption behavior impacts the electrical conductivity of the material. The HOMO and LUMO distributions for the Pd-BN monolayer, Rh-BN monolayer, and the adsorption systems of three gases on different monolayers are shown in Figure 7.

From Figure 7, it can be observed that before adsorption the HOMO and LUMO of the Pd-BN and Rh-BN systems are primarily localized around the dopant atoms. After gas adsorption, the distributions of HOMO and LUMO shift significantly. The HOMO becomes predominantly localized near the gas molecules, while the LUMO begins to interact with the BN monolayer. This change is likely due to electron redistribution induced by gas adsorption.

The bandgap values for each system can be calculated based on the energies of the HOMO and LUMO. Consistent with the conclusions from the density of states analysis, the bandgaps of the systems with adsorbed H_2, CH_4, and C_2H_4 gases are increased compared to their non-adsorbed counterparts. The effect of CH_4 adsorption on the bandgap of Pd-BN and Rh-BN monolayers is less pronounced, which aligns with the results obtained from the density of states analysis.

Response recovery characteristics

For gas sensors, the desorption time is a crucial parameter for assessing the repeatability of the sensor. According to the Van't Hoff-Arrhenius expression, the desorption time can be calculated using the following Formula 5.

$$\tau = A^{-1} e^{-E_\alpha/(k_B T)} \tag{5}$$

In the formula, A represents the attempt frequency ($A = 10^{12} \cdot s^{-1}$), T is the temperature; k_B represents the Boltzmann constant ($k_B = 8.62 \times 10^{-5}$eV/K); E_α is the activation energy required for desorption, assumed to be the same as E_{ads}. The desorption times of H_2, CH_4, and C_2H_4 at temperatures of 298 K,

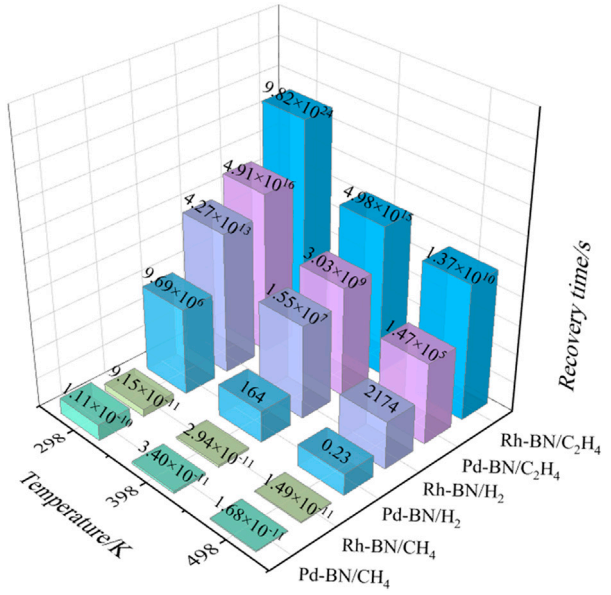

FIGURE 8
Desorption time of three gas molecules from the Pd-BN monolayer and Rh-BN monolayer.

398 K, and 498 K from the surfaces of Pd-BN and Rh-BN monolayers are illustrated in Figure 8.

As illustrated in Figure 8, the desorption times for CH_4 molecules from both Pd-BN and Rh-BN monolayers are remarkably brief, with corresponding adsorption energies of −0.121 eV and −0.116 eV, respectively. These short desorption times suggest that CH_4 exhibits a very low likelihood of being effectively adsorbed by either the Pd-BN or Rh-BN monolayers, rendering it unsuitable as a target gas for sensors utilizing these materials. In contrast, H_2 molecules demonstrate more favorable desorption characteristics from the Pd-BN monolayer, requiring only 164 s at 398 K. This indicates that the Pd-BN monolayer is particularly well-suited for the development of sensitive materials for H_2 gas detection.

Conversely, for C_2H_4, even at elevated temperatures of 498 K, the desorption times from both Pd-BN and Rh-BN monolayers remain inadequate. Given that C_2H_4 is a known carcinogen and poses risks to both atmospheric quality and water sources, there is potential for the Pd-BN and Rh-BN monolayers to be utilized as effective adsorbents for the remediation of C_2H_4 gas.

Comparison of gas adsorption characteristics of h-BN with Pd-BN and Rh-BN monolayers

This study compares the adsorption performance of dissolved characteristic gases in oil on Pd-BN monolayers, Rh-BN monolayers, and native h-BN. It further investigates the potential of h-BN monolayers as gas-sensing materials in the power industry.

The comparison results are presented in Table 2. The intrinsic h-BN exhibits suboptimal adsorption characteristics for dissolved target gases such as H_2, CH_4, and C_2H_4 in oil compared to the doped Pd-BN and Rh-BN monolayers. Both the absolute values of the adsorption energies and charge transfer amounts are relatively low, with larger adsorption distances, indicating that intrinsic h-BN is not sensitive to H_2, CH_4, and C_2H_4.

TABLE 2 Comparison of adsorption characteristics of h-BN with Pd-BN and Rh-BN monolayers.

Adsorption system	Gas	E_{ads} (eV)	Q_t (e)	D(Å)
Pd-BN	H_2	−1.123	−0.044	1.736
	CH_4	−0.121	−0.028	1.968
	C_2H_4	−1.697	−0.100	2.157
Rh-BN	H_2	−1.516	−0.027	1.686
	CH_4	−0.116	0.028	1.886
	C_2H_4	−2.188	−0.090	2.120
h-BN	H_2	−0.070	−0.004	3.014
	CH_4	−0.072	−0.013	3.038
	C_2H_4	−0.102	−0.007	3.320

In contrast, the adsorption energies for the various gas systems are significantly increased in both Pd-BN and Rh-BN compared to intrinsic h-BN, particularly for H_2 and C_2H_4, which show stronger chemisorption effects. Both doped monolayers exhibit a strong capture capability for C_2H_4, with a tendency for reduced desorption. Among the doped variants, Pd-BN demonstrates a superior desorption effect for H_2 compared to Pd-BN, with a recovery time of 164 s at 398 K, making Pd-BN more favorable as a hydrogen-sensitive material. Doping with Pd or Rh atoms effectively enhances the gas-sensing performance of h-BN monolayers for dissolved target gases in oil, proving to be an effective modification strategy.

Conclusion

This study constructed models of Pd-doped and Rh-doped h-BN monolayers to analyze their adsorption characteristics for H_2, CH_4, and C_2H_4 gases found in transformer oil. The findings demonstrate that both Pd-BN and Rh-BN monolayers exhibit strong chemical adsorption for H_2 and C_2H_4, characterized by high adsorption energies, short distances, and significant charge transfer, while their interaction with CH_4 is primarily governed by van der Waals forces. Notably, Pd-BN and Rh-BN monolayers showed reduced electrical conductivity after gas adsorption, highlighting their suitability for gas detection; the Pd-BN monolayer, in particular, has a desorption time of only 164 s for H_2 at 398 K, indicating its potential in hydrogen sensing applications. Furthermore, the incorporation of Pd and Rh enhances the adsorption energy and charge transfer capabilities compared to intrinsic h-BN, positioning these materials as promising candidates for dissolved gas sensors in transformer oils and providing a solid theoretical basis for future development.

Data availability statement

The original contributions presented in the study are included in the article/supplementary material, further inquiries can be directed to the corresponding author.

Author contributions

JJ: Conceptualization, Writing–original draft, Writing–review and editing. DY: Supervision, Writing–review and editing. WZ: Conceptualization, Data curation, Supervision, Writing–review and editing. ZW: Data curation, Supervision, Writing–review and editing. QZ: Funding acquisition, Supervision, Writing–review and editing.

Funding

The author(s) declare that financial support was received for the research, authorship, and/or publication of this article. This research was funded by the National Natural Science Foundation of China, grant number 52077177.

Conflict of interest

The authors declare that the research was conducted in the absence of any commercial or financial relationships that could be construed as a potential conflict of interest.

The reviewer WC declared a shared affiliation with the author WZ at the time of review.

The author(s) declared that they were an editorial board member of Frontiers, at the time of submission. This had no impact on the peer review process and the final decision.

Generative AI statement

The author(s) declare that no Generative AI was used in the creation of this manuscript.

Publisher's note

References

Ali, M. S., Bakar, A. A., Omar, A., Jaafar, A. S. A., and Mohamed, S. H. (2023). Conventional methods of dissolved gas analysis using oil-immersed power transformer for fault diagnosis: a review. *Electr. Power Syst. Res.* 216, 109064. doi:10.1016/j.epsr.2022.109064

Bustamante, S., Manana, M., Arroyo, A., Castro, P., Laso, A., and Martinez, R. (2019). Dissolved gas analysis equipment for online monitoring of transformer oil: a review. *Sensors* 19, 4057. doi:10.3390/s19194057

Chen, D. C., Li, Y., Xiao, S., Yang, C. X., Zhou, J., and Xiao, B. B. (2022). Single Ni atom doped WS2 monolayer as sensing substrate for dissolved gases in transformer oil: a first-principles study. *Appl. Surf. Sci.* 579, 152141. doi:10.1016/j.apsusc.2021.152141

Chen, F. Y., Hong, C. X., Jiang, J. M., Zhang, Z. Y., and Zhou, Q. (2024). A comparative DFT study on the adsorption properties of lithium batteries thermal runaway gases CO, CO2, CH4 and C2H4 on pristine and Au doped CdS monolayer. *Surfaces Interfaces* 46, 104200. doi:10.1016/j.surfin.2024.104200

Du, L., Wang, Y. B., Wang, W. J., and Chen, X. X. (2018). Studies on a thermal fault simulation device and the pyrolysis process of insulating oil. *Energies* 11, 3392. doi:10.3390/en11123392

Du, R. J., and Wu, W. (2022). Adsorption of gas molecule on Rh, Ru doped monolayer MoS2 for gas sensing applications: a DFT study. *Chem. Phys. Lett.* 789, 139300. doi:10.1016/j.cplett.2021.139300

Elele, U., Nekahi, A., Arshad, A., and Fofana, I. (2022). Towards online ageing detection in transformer oil: a review. *Sensors* 22, 7923. doi:10.3390/s22207923

Gao, J., Chen, F. J., Xue, C. W., Hu, C. C., and Lin, L. (2024). Adsorption behavior of Rh-VSe2 monolayer upon dissolved gases in transformer oil and the effect of applied electric field. *Flatchem* 47, 100706. doi:10.1016/j.flatc.2024.100706

Gao, M. Y., Ren, Q. Q., Wang, Z. X., Wang, S. M., Ning, T. G., Ma, X. L., et al. (2024). Fast response 2D semiconductor gas sensor for memory-type NO2 detection: test system construction, performance evaluation, and mechanism study. *Mater. Sci. Semicond. Process.* 174, 108249. doi:10.1016/j.mssp.2024.108249

Grimme, S. (2006). Semiempirical GGA-type density functional constructed with a long-range dispersion correction. *J. Comput. Chem.* 27 (15), 1787–1799. doi:10.1002/jcc.20495

Guo, L. Y., Xia, S. Y., Long, Y. F., Peng, Z. R., Tan, Y. X., Jiang, T. Y., et al. (2022). P-doped h-BN monolayer: a high-sensitivity SF_6 decomposition gases sensor. *Ieee Sensors J.* 22 (19), 18281–18286. doi:10.1109/Jsen.2022.3193873

Hussein, T. A., Shiltagh, N. M., Alaarage, W. K., Abbas, R. R., Jawad, R. A., and Nasria, A. H. A. (2023). Electronic and optical properties of the BN bilayer as gas sensor for CO2, SO2, and NO2 molecules: a DFT study. *Results Chem.* 5, 100978. doi:10.1016/j.rechem.2023.100978

Jiang, T. Y., Xie, H. A., Wu, H., Chen, L., Bi, M. Q., and Chen, X. (2024). Adsorption of dissolved gases (CO, H2, CO2) produced by partial discharge in converter transformer oil by CuO(1, 2) and Ag2O(1, 2) clusters doped with MoTe2: a DFT study. *Mater. Today Commun.* 40, 109637. doi:10.1016/j.mtcomm.2024.109637

Kou, X. Y., Xie, N., Chen, F., Wang, T. S., Guo, L. L., Wang, C., et al. (2018). Superior acetone gas sensor based on electrospun SnO2 nanofibers by Rh doping. *Sensors Actuators B-Chemical* 256, 861–869. doi:10.1016/j.snb.2017.10.011

Kumar, S., Mirzaei, A., Kumar, A., Lee, M. H., Ghahremani, Z., Kim, T. U., et al. (2024). Nanoparticles anchored strategy to develop 2D MoS2 and MoSe2 based room temperature chemiresistive gas sensors. *Coord. Chem. Rev.* 503, 215657. doi:10.1016/j.ccr.2024.215657

Li, B. L., Zhou, Q., Liu, Y. P., and Chen, J. X. (2022). A novel nondestructive testing method for dielectric loss factor of transformer oil based on multifrequency ultrasound. *Ieee Trans. Dielectr. Electr. Insulation* 29 (5), 1659–1665. doi:10.1109/Tdei.2022.3190821

Li, Z. H., Jia, L. F., Chen, J. X., Cui, X. S., and Zhou, Q. (2022). Adsorption and sensing performances of pristine and Au-decorated gallium nitride monolayer to noxious gas molecules: a DFT investigation. *Front. Chem.* 10, 898154. doi:10.3389/fchem.2022.898154

Long, Y. F., Peng, Z. Y., Guo, L. Y., He, X. H., Zhu, M. Y., Yang, Z. W., et al. (2024). Adsorption behavior of dissolved gas molecules in transformer oil on Rh modified GeSe monolayer. *Acs Omega* 9 (6), 7061–7068. doi:10.1021/acsomega.3c09001

Manoj, T., Ranga, C., Ghoneim, S. S. M., Rao, U. M., and Abdelwahab, S. A. M. (2023). Alternate and effective dissolved gas interpretation to understand the transformer incipient faults. *Ieee Trans. Dielectr. Electr. Insulation* 30 (3), 1231–1239. doi:10.1109/Tdei.2023.3237795

Mishra, M., Dash, A., Sharma, A., Khanuja, M., and Gupta, G. (2022). CO sensing properties of nanostructured WSe2/GaN and MoSe2/GaN based gas sensors. *Phys. E-Low-Dimensional Syst. and Nanostructures* 139, 115147. doi:10.1016/j.physe.2022.115147

Mu, L., Chen, D. C., and Cui, H. (2022). Single Pd atom embedded Janus HfSeTe as promising sensor for dissolved gas detection in transformer oil: a density functional theory study. *Surfaces Interfaces* 35, 102398. doi:10.1016/j.surfin.2022.102398

Ngamprapawat, S., Kawase, J., Nishimura, T., Watanabe, K., Taniguchi, T., and Nagashio, K. (2023). From *h*BN to graphene: characterizations of hybrid carbon doped *h*BN for applications in electronic and optoelectronic devices. *Adv. Electron. Mater.* 9 (8). doi:10.1002/aelm.202300083

Ni, J. M., Wang, W., Quintana, M., Jia, F. F., and Song, S. X. (2020). Adsorption of small gas molecules on strained monolayer WSe2 doped with Pd, Ag, Au, and Pt: a computational investigation. *Appl. Surf. Sci.* 514, 145911. doi:10.1016/j.apsusc.2020.145911

Ogawa, S., Fukushima, S., and Shimatani, M. (2023). Hexagonal boron nitride for photonic device applications: a review. *Materials* 16, 2005. doi:10.3390/ma16052005

Oyo-Ita, I., Louis, H., Nsofor, V. C., Edet, H. O., Gber, T. E., Ogungbemiro, F. O., et al. (2023). Studies on transition metals (Rh, Ir, Co) doped silicon carbide nanotubes (SiCNT) for the detection and adsorption of acrolein: insight from DFT approach. *Mater. Sci. Eng. B-Advanced Funct. Solid-State Mater.* 296, 116668. doi:10.1016/j.mseb.2023.116668

Peng, R. C., Zeng, W., and Zhou, Q. (2023). Adsorption and gas sensing of dissolved gases in transformer oil onto Ru3-modified SnS2: a DFT study. *Appl. Surf. Sci.* 615, 156445. doi:10.1016/j.apsusc.2023.156445

Peng, R. C., Zhou, Q., and Zeng, W. (2021). First-principles insight into Pd-doped C3N monolayer as a promising scavenger for NO, NO2 and SO2. *Nanomaterials* 11, 1267. doi:10.3390/nano11051267

Sun, N., Tian, Q. Y., Bian, W. A., Wang, X., Dou, H. R., Li, C. J., et al. (2023). Highly sensitive and lower detection-limit NO2 gas sensor based on Rh-doped ZnO nanofibers prepared by electrospinning. *Appl. Surf. Sci.* 614, 156213. doi:10.1016/j.apsusc.2022.156213

Tang, S. R., Chen, W. G., Jin, L. F., Zhang, H., Li, Y. Q., Zhou, Q., et al. (2020). SWCNTs-based MEMS gas sensor array and its pattern recognition based on deep belief networks of gases detection in oil-immersed transformers. *Sensors Actuators B-Chemical* 312, 127998. doi:10.1016/j.snb.2020.127998

Wang, J. C., Zhang, X. X., Liu, L., and Wang, Z. T. (2021). Dissolved gas analysis in transformer oil using Ni-Doped GaN monolayer: a DFT study. *Superlattices Microstruct.* 159, 107055. doi:10.1016/j.spmi.2021.107055

Wang, J. G., Ma, F. C., Liang, W. J., and Sun, M. T. (2017). Electrical properties and applications of graphene, hexagonal boron nitride (h-BN), and graphene/h-BN heterostructures. *Mater. Today Phys.* 2, 6–34. doi:10.1016/j.mtphys.2017.07.001

Wang, Y. J., Yao, J. N., Zhou, Q. X., Su, D. T., Ju, W. W., and Wang, L. Y. (2024). Transition-metal doped Ti2CO2 as gas sensor toward NH3: a DFT study. *Chem. Phys.* 586, 112376. doi:10.1016/j.chemphys.2024.112376

Wu, H., Fang, J., Yuan, S., Liu, Y. P., Zeng, J. F., and Jiang, T. Y. (2024). Exploration on the application of copper oxide particles doped janus ZrSSe in detecting dissolved gases in oil-immersed transformers: a DFT study. *Mater. Today Chem.* 38, 102038. doi:10.1016/j.mtchem.2024.102038

Yao, G. Y., Zou, W. J., Yu, J., Zhu, H. C., Wu, H., Huang, Z. X., et al. (2024). Pd/PdO doped WO3 with enhanced selectivity and sensitivity for ppb level acetone and ethanol detection. *Sensors Actuators B-Chemical* 401, 135003. doi:10.1016/j.snb.2023.135003

Yu, P., Zhang, M. Y., You, M. Q., Gao, Y. X., Xiao, L. D., Peng, Y., et al. (2024). Pd doped Janus HfSeS monolayer: ultrahigh sensitive gas sensing material for reversible detection of NO. *Sensors Actuators a-Physical* 365, 114864. doi:10.1016/j.sna.2023.114864

Zeng, F. P., Wu, S. Y., Lei, Z. C., Li, C., Tang, J., Yao, Q., et al. (2020). SF6 fault decomposition feature component extraction and triangle fault diagnosis method. *Ieee Trans. Dielectr. Electr. Insulation* 27 (2), 581–589. doi:10.1109/Tdei.2019.008370

Zhang, J. Q., Li, T. X., Zhang, H. M., Huang, Z. W., Zeng, W., and Zhou, Q. (2024). Ni decorated ReS2 monolayer as gas sensor or adsorbent for agricultural greenhouse gases NH3, NO2 and Cl2: a DFT study. *Mater. Today Chem.* 38, 102114. doi:10.1016/j.mtchem.2024.102114

Zhang, X. X., Fang, R. X., Chen, D. C., and Zhang, G. Z. (2019). Using Pd-doped γ-graphyne to detect dissolved gases in transformer oil: a density functional theory investigation. *Nanomaterials* 9, 1490. doi:10.3390/nano9101490

Zhao, C. J., and Wu, H. R. (2018). A first-principles study on the interaction of biogas with noble metal (Rh, Pt, Pd) decorated nitrogen doped graphene as a gas sensor: a DFT study. *Appl. Surf. Sci.* 435, 1199–1212. doi:10.1016/j.apsusc.2017.11.146

Zhong, M. W., Cao, Y. F., He, G. L., Feng, L. T., Tan, Z. C., Mo, W. J., et al. (2023). Dissolved gas in transformer oil forecasting for transformer fault evaluation based on HATT-RLSTM. *Electr. Power Syst. Res.* 221, 109431. doi:10.1016/j.epsr.2023.109431

Zhou, Q., Xu, L. N., Umar, A., Chen, W. G., and Kumar, R. (2018). Pt nanoparticles decorated SnO2 nanoneedles for efficient CO gas sensing applications. *Sensors Actuators B-Chemical* 256, 656–664. doi:10.1016/j.snb.2017.09.206

Zhou, X., Tian, T., Liu, N. B., Bai, J., Luo, Y., Li, X. G., et al. (2023). Research on gas production law of free gas in oil-immersed power transformer under discharge fault of different severity. *Front. Energy Res.* 10. doi:10.3389/fenrg.2022.1056604